



RESEARCH ARTICLE

New data fails to replicate the small-scale radiocarbon anomalies in the early second millennium CE

A Scifo¹, T Abi Nassif¹, M Conti¹, A Bayliss², P Doeve³ and M W Dee¹

¹Centre for Isotope Research, University of Groningen, Groningen, The Netherlands, ²Historic England, London, United Kingdom and ³BAAC B.V., 's Hertogenbosch, The Netherlands

Corresponding author: A. Scifo; Email: a.scifo@rug.nl

Received: 17 July 2023; **Revised:** 20 March 2024; **Accepted:** 26 March 2024

Keywords: cosmic radiation events; radiocarbon production

Abstract

Over the last decade, the field of radiocarbon analysis has been revolutionized by the discovery of single-year anomalies, because they can be used as markers of space weather events and as time anchors for exact dating. Brehm et al. (2021) recently analyzed two new anomalies, in the years 1052 CE and 1279 CE. These candidates show consecutive year $\Delta^{14}\text{C}$ increases of 5.9‰ and 6.5‰, respectively. In this study, we measured and analyzed dendrochronologically dated oak wood samples from northern Europe spanning both these years. Our results, although statistically consistent with those presented in the original publication, show effectively no increase in $\Delta^{14}\text{C}$ (1 and 2.5 times the measurement error, respectively). Nonetheless, we proceed to analyze our datasets with the aid of the open-source Python package `ticktack`. Our modeled outputs confirm that radiocarbon production barely rose above background levels across these two periods, and no event of clearly resolvable start date or duration could be detected. Additionally, we conduct the same analyses on a new sample spanning the years 531–550 CE. Here, once again, only weak evidence was obtained for any increase in radiocarbon production, and no significant annual rise was evident. The gradual increases exhibited by all three of these samples, and the ubiquity of these patterns across the calibration curve, call into question any likely cosmic event in these cases, and illustrate how challenging it will be to distinguish lower magnitude events in the radiocarbon record.

Introduction

Radiocarbon (^{14}C) is a cosmogenic nuclide produced in the upper layers of the atmosphere via interaction between cosmic radiation and nitrogen atoms. Its formation rate is dependent on several factors, with the flux of cosmic rays (highly energetic particles) being the main driver. The incoming cosmic rays set in train a particle shower that ultimately leads to the generation of thermal neutrons which are captured by nitrogen atoms to form ^{14}C (Beer et al. 2012; Lingenfelter 1963; Simpson 1951). Under normal conditions, it is estimated that the incoming radiation ultimately responsible for ^{14}C formation has almost entirely a galactic origin, and only 0.25% has a solar origin in the form of solar energetic particles (SEP) (Kovaltsov et al. 2012). On average, galactic cosmic rays (GCR) are several orders of magnitude more energetic than SEPs; therefore, despite their much lower fluence, they are more likely to penetrate the magnetic shielding of the Earth and to initiate the nuclear spallation processes (Beer et al. 2012; Kovaltsov et al. 2012). The activity of the Sun also plays a fundamental role. Specifically, the heliomagnetic and geomagnetic fields and their interaction dictate which fraction of the incoming radiation will be able to penetrate the resulting magnetic shielding and enter the atmosphere. It is when the Sun is at its maximum activity and the Earth's magnetic shield is also intensified that ^{14}C production is at its minimum (Damon et al. 1973; Damon and Linick 1986; Stuiver 1961; Stuiver and Braziunas 1993). However, the Sun often also exhibits violent behavior, which sporadically results in

flares or coronal mass ejections (CMEs) that liberate into interplanetary space intense fluxes of SEPs, orders of magnitude more energetic than ordinary solar cosmic rays (Kovaltsov et al. 2012; Usoskin 2017). When such SEPs hit Earth, they could trigger exceptional production of cosmogenic nuclides, even though the direct observational evidence of this phenomenon is limited (Paleari et al. 2023; Pedro et al. 2012; Usoskin et al. 2020). For instance, the strongest solar storm that happened to hit the Earth in recent history, the Carrington Event of 1859 CE, left no trace in available cosmogenic nuclide records (McCracken et al. 2001; Scifo et al. 2019; Smart et al. 2006; Wolff et al. 2012).

Sudden increases in the ^{14}C content of known-age tree rings were first discovered by Miyake et al. (Miyake et al. 2012, 2013) and have been commonly referred to as Miyake Events, but also as rapid ^{14}C changes or ^{14}C production events in the scientific literature. As these anomalous uplifts are observed all over the world, they cannot be considered the outcome of some regional phenomena but instead they must be analyzed at a global scale. The origin of rapid ^{14}C changes has been linked to extreme solar activity (Mekhaldi et al. 2015; Melott and Thomas 2012; Usoskin et al. 2013). Although no consensus yet exists over the mechanism for such explosive solar behavior, some form of CME is believed to be the most likely explanation, as any correlation with astrophysical gamma ray sources appears to be weak (Dee et al. 2016; Terrasi et al. 2020). Furthermore, the latter phenomenon would also not produce major increases in ^{10}Be (Pavlov et al. 2013), yet the most widely accepted events have been found in ice core records of ^{10}Be and ^{36}Cl (Mekhaldi et al. 2015; O'Hare et al. 2019; Paleari et al. 2022).

Recently, the ^{14}C production events in both 775 CE and 993 CE have been used as linchpins for ^{14}C dating. Since their occurrence has been exactly pinpointed in time, by way of numerous dendrochronological archives (Büntgen et al. 2018), they can be used as reliable time anchors to provide exact-year dates. The first application of this sort confirmed the construction date of a church in Switzerland (Wacker et al. 2014), this was followed by dates for the Changbaishan and Katla volcanic eruptions (Büntgen et al. 2017; Oppenheimer et al. 2017), then an archeological site in Russia (Kuitems et al. 2020), and most recently the arrival of Europeans in North America (Kuitems et al. 2022).

Uncovering new rapid ^{14}C changes is an area of active research. Multiple criteria need to be met in order for new candidates to be accepted as true events. Firstly, the measurement data need to be sufficiently precise to distinguish them from adjacent (background) data, as well as generic solar and carbon cycle induced fluctuations. Secondly, the data should be corroborated by measurements on different trees, ideally of more than one species, from more than one geographic location, and by more than one ^{14}C laboratory ([Büntgen et al. 2018] c.f. (Wang et al. 2017; Jull et al. 2021)). Additional support must also be obtained from data on other cosmogenic isotopes, ^{10}Be and ^{36}Cl , from ice cores, as the $^{36}\text{Cl}/^{10}\text{Be}$ ratio is a good discriminator for the energy of incoming cosmic rays (Mekhaldi et al. 2015; Webber et al. 2007). Brehm et al. (2021) have analyzed two new event candidates relating to the years 1052 and 1279 CE, respectively. The 1052 CE event candidate was first proposed by Terrasi et al. (2020), although here the increase was observed in the year 1054 CE, and it was argued that the Crab Nebula supernova, documented in historical accounts in the same year, could have been the cause for the feature. Panyushkina et al. (2022) pointed to the dating discrepancy between the oak tree-ring series used by Brehm et al. (2021) and Terrasi et al. (2020) and applied DTW analysis to four ^{14}C signatures from tree rings of California, Finland, and England and suggested that the two ^{14}C features reported by the two studies could have been caused by a single event. These event candidates studied by Brehm et al. (2021) show a relatively small increase in $\Delta^{14}\text{C}$ compared to other events, such as the ones already used for single-year dating. In this study, we aim to corroborate the findings of Brehm et al. (2021) by using independent tree ring samples dendrochronologically dated to the periods of time in question. We also report a new investigation into an anomalous $\Delta^{14}\text{C}$ rise in the 540s CE, and new measurements over the 775 CE event.

In order to interpret changes in $^{14}\text{C}/^{12}\text{C}$ ratio in wood samples correctly, and to link them with space weather events, the ^{14}C data must first be passed through a model of the carbon cycle, as atmospheric $^{14}\text{C}/^{12}\text{C}$ ratio depends on the mixing between reservoirs with different sizes and residence times, leading to a mismatch between $\Delta^{14}\text{C}$ changes and ^{14}C production rate changes. The most common way to do so is using Carbon Box Models (CBM) (Oeschger et al. 1975; Siegenthaler et al. 1980; Nakamura et al. 1987).

This has been done by several studies that have reported new event candidates, using in-house CBMs. However, none of those CBMs are in the public domain and therefore they are inaccessible to other research groups, making the comparison between proven and candidate events more difficult and controversial. Consequently, we welcome the release of the open-source Python package, `ticktack`, which encompasses CBM implementations with modern Bayesian inference tools (Zhang et al. 2022). The package allows the user to either implement one of the previously employed CBMs (Büntgen et al. 2018; Brehm et al. 2021; Güttler et al. 2015; Miyake et al. 2012) or to custom build one of your own.

Methods

Samples Preparation and Measurement

In this study, we analyze four different dendrochronologically dated wood samples, all of which are oak (*Quercus* sp.). Sample BIF-E19, spanning the years 1049–1057 CE, comes from Furness Abbey [54°8'7"N, 3°11'52"W], England. Sample APT-C02, spanning the years 1275–1283 CE, comes from Apethorpe Church [52°32'59"N, 0°29'29"W], England. Sample 14.0123.121, spanning the years 531–550 CE, comes from a plank from a water well found during archaeological excavations near present day Ruiselede [51°2'0"N, 03°23'0"E], Belgium (Doeve 2017). Sample D1600030, spanning the years 771–779 CE, comes from the archaeological site of Dorestad [51°58'30"N, 5°20'24"E], The Netherlands (Doeve and Jansma 2023). The former two samples were provided by Historic England, the second sample by the Dendrochronology Laboratory at BAAC, the fourth sample by the Cultural Heritage Agency of the Netherlands. For additional details, see Supplementary Information (S15 and S16). All the samples were first carefully dissected into single-year whole growth rings under a light microscope, including both early wood and late wood, and subsequently the α -cellulose fraction was extracted through a wet chemistry procedure (see Dee et al. (2020)). The α -cellulose products were combusted to CO₂, which was then trapped and graphitized in accordance with the routine procedures of the Centre for Isotope Research (CIO), University of Groningen (see Dee et al. 2020). The graphite samples were finally analyzed for their ¹⁴C content by accelerator mass spectrometry (AMS) utilizing the IonPlus MICADAS system at CIO (Dee et al. 2020; Aerts-Bijma et al. 2021). Samples BIF-E19 and APT-C02 had tree rings big enough to allow measurement of each annual sample in duplicate, in separate batches. The same procedure was only possible for a few tree rings in the case of sample 14.0123.121, while it was not possible at all for sample D1600030. These duplicate measurements are ones where the whole preparation process was entirely repeated, from wood to measurement.

Data Analysis

After obtaining the ¹⁴C/¹²C ratio of each ring, the rings measured in duplicate are tested for compatibility through the χ^2 -test performed at 95% probability (or at 5% significance level). Then the averaged results, expressed in terms of $\Delta^{14}\text{C}$, are modeled as short time series in the Python package `ticktack`. As stated above, this package allows the user to specify their own carbon reservoir sizes and fluxes, or to re-implement one of four models utilized in recent publications, namely the 3-box model of Miyake et al. (2012), the 11-box model of Güttler et al. (2015) or the 22-box models of Büntgen et al. (2018) and Brehm et al. (2021). In this study, we chose to analyze all our datasets using the 22-box model from Brehm et al. (2021). This decision also allowed us to compare our results directly with the ones obtained by the study proposing the new events. For more details on the structure of this box-model, see (Brehm et al. 2021). To reconstruct ¹⁴C production rates, we load the $\Delta^{14}\text{C}$ time series together with the chosen CBM as a `SingleFitter` object, which can perform parametric Bayesian inference of ¹⁴C production rates for single data sets, where the sampling engine is `emcee`, an MIT-licensed implementation of the Affine Invariant MCMC Ensemble sampler (Goodman and Weare 2010). As three of the four datasets are shorter than twice the typical duration of the Schwabe cycle, it is

not possible to fit a sinusoid to the production rate before the event candidates; therefore, we first apply the method `spike only`, which assumes a flat production rate for the years prior to the putative spike. Later, we apply the method `flexible sinusoid affine variant`, which fits a sinusoid and a trend to the data.

The model estimates various parameters of which the ^{14}C production rate can be expressed as a function. The parameters inferred by the `spike only` method are *Start Date* (in years), *Duration* (in years) and *Area* (in atoms/cm² year/s), where the latter one refers to the area under that super-Gaussian curve, that is the total ^{14}C production under the integrated time period (Zhang et al. 2022). The method `flexible sinusoid affine variant`, apart from inferring parameters such as *Start Date*, *Duration* and *Area* of the possible event, infers other parameters, such as *Gradient*, *Phi*, and *Amplitude*. It allows the model to fit the data to a sinusoid of phase *Phi* and amplitude *Amplitude*, and a trend given by the parameter *Gradient*. For both these methods, initial values for these parameters are estimated, and then the engine jointly scans them within a defined boundary in order to best fit the data. The exact detail of the sampling is defined by the number of burn-in and production steps. For more information on the functioning and structure of the package, see Zhang et al. (2022).

Results and Discussion

In Table 1, the averaged results for the four different wood samples are presented in the $\Delta^{14}\text{C}$ format. Every duplicate measurement on every sample agrees, passing the χ^2 -test at 5% significance level, and therefore can be averaged. See Tables 1-SI, 2-SI, 3-SI and Figures 1-SI, 2-SI and 3-SI in Supplementary Information (SI1) for a more detailed presentation of all the measurements.

Firstly, we present new ^{14}C measurements over the period from 771–779 CE, spanning the years of the 775 CE event. Our results show the same sharp rise shown by Miyake et al. (2012), even though the $\Delta^{14}\text{C}$ values are on average higher than the ones reported from the original study. Our results do not appear to be anomalous when compared with all the data from the Northern Hemisphere reported by the survey over this event by Büntgen et al. (2018) (Figure 1A). We also observe that the $\Delta^{14}\text{C}$ rise spans a two-year period; this has been observed before in some datasets, although it is still not clear what causes a difference between a sharp and a prolonged rise for this event, as both phenomenologies can be seen in trees from different locations and growing conditions (Büntgen et al. 2018; Zhang et al. 2022).

Regarding the 1052 CE event candidate, our results across sample BIF-E19 are directly compared with those published by Brehm et al. (2021) (Figure 2A). Brehm et al. (2021) measured a $\Delta^{14}\text{C}$ increase of $5.9 \pm 1.1\%$ between the calendar years 1052 and 1053 CE, and points to a possible connection between such an increase and an SEP event. All the data points of our time series agree with those of Brehm et al. (2021) at 1σ probability, apart from the points at 1052 and 1057 CE, which are nevertheless consistent at 2σ probability; indeed all the sets of same-year measurements pass the χ^2 -test at 5% significance level. Thus, our results are statistically compatible with Brehm et al. (2021), and both data sets can also be averaged (see Supplementary Information, SI2). Looking at the results from our study alone, we could point to a slight increase in $\Delta^{14}\text{C}$ between the years 1054 and 1055 CE, namely of $4.4 \pm 1.7\%$. Such an increase is only around two and a half times the measurement error, and so would routinely be regarded as negligible. However, it is somewhat comparable to the increase inferred by Brehm et al. (2021) between 1052 and 1053 CE, although not co-eval. This temporal disparity was also found between Brehm et al. (2021) and Terrasi et al. (2020). However, Panyushkina et al. (2022), performing DTW analyses over ^{14}C time series, points out that those two features are possibly one and the same. In Supplementary Information 3 (SI3) we briefly show that even if one hypothesizes that there was a mistake in one of the dendrochronologies, the two datasets are still statistically compatible.

Regarding the 1279 CE event candidate, our results over sample APT-C02 are directly compared with the results published by Brehm et al. (2021) (Figure 3A). Brehm et al. (2021) measured a $\Delta^{14}\text{C}$ increase of $6.5 \pm 1.6\%$ between the calendar years 1279 and 1280 CE, again suggesting a possible

Table 1. Averaged $\Delta^{14}\text{C}$ results and errors obtained on the four wood samples

| Sample | Calendar year (CE) | Duplicate measurement | $\Delta^{14}\text{C}$ (‰) | $\pm \sigma$ (‰) |
|-------------|--------------------|-----------------------|---------------------------|------------------|
| BIF-E19 | 1049 | Yes | -7.05 | 2.08 |
| | 1050 | Yes | -5.03 | 1.84 |
| | 1051 | Yes | -8.53 | 1.53 |
| | 1052 | Yes | -6.24 | 2.16 |
| | 1053 | Yes | -7.31 | 2.32 |
| | 1054 | Yes | -6.25 | 2.08 |
| | 1055 | Yes | -1.81 | 1.88 |
| | 1056 | Yes | -2.77 | 1.75 |
| | 1057 | Yes | -2.92 | 2.08 |
| APT-C02 | 1275 | Yes | -14.46 | 1.76 |
| | 1276 | Yes | -13.50 | 1.64 |
| | 1277 | Yes | -13.48 | 1.64 |
| | 1278 | Yes | -12.95 | 1.64 |
| | 1279 | Yes | -11.33 | 1.71 |
| | 1280 | Yes | -9.60 | 1.59 |
| | 1281 | Yes | -11.35 | 1.69 |
| 14.0123.121 | 1282 | Yes | -11.36 | 1.57 |
| | 1283 | Yes | -9.44 | 1.71 |
| | 531 | No | -25.02 | 1.91 |
| | 532 | No | -22.16 | 1.74 |
| | 533 | No | -23.20 | 1.78 |
| | 534 | No | -22.51 | 1.89 |
| | 535 | No | -22.65 | 1.70 |
| | 536 | No | -23.18 | 1.74 |
| | 537 | Yes | -23.75 | 1.38 |
| | 538 | Yes | -23.39 | 1.37 |
| | 539 | No | -22.93 | 1.79 |
| | 540 | Yes | -23.39 | 1.37 |
| | 541 | Yes | -23.35 | 1.43 |
| | 542 | Yes | -21.31 | 1.39 |
| | 543 | No | -19.43 | 1.71 |
| 544 | Yes | -19.88 | 1.44 | |
| 545 | No | -17.87 | 1.80 | |
| 546 | No | -17.06 | 1.89 | |
| 547 | No | -19.92 | 1.82 | |
| 548 | No | -19.03 | 1.84 | |
| 549 | Yes | -20.85 | 1.38 | |
| 550 | Yes | -19.69 | 1.43 | |
| D1600030 | 771 | No | -20.44 | 1.93 |
| | 772 | No | -18.57 | 1.95 |
| | 773 | No | -21.15 | 1.92 |
| | 774 | No | -17.30 | 1.94 |
| | 775 | No | -7.65 | 1.98 |
| | 776 | No | 1.67 | 1.97 |
| | 777 | No | -2.93 | 2.01 |
| | 778 | No | -4.12 | 1.98 |
| | 779 | No | -4.27 | 1.96 |

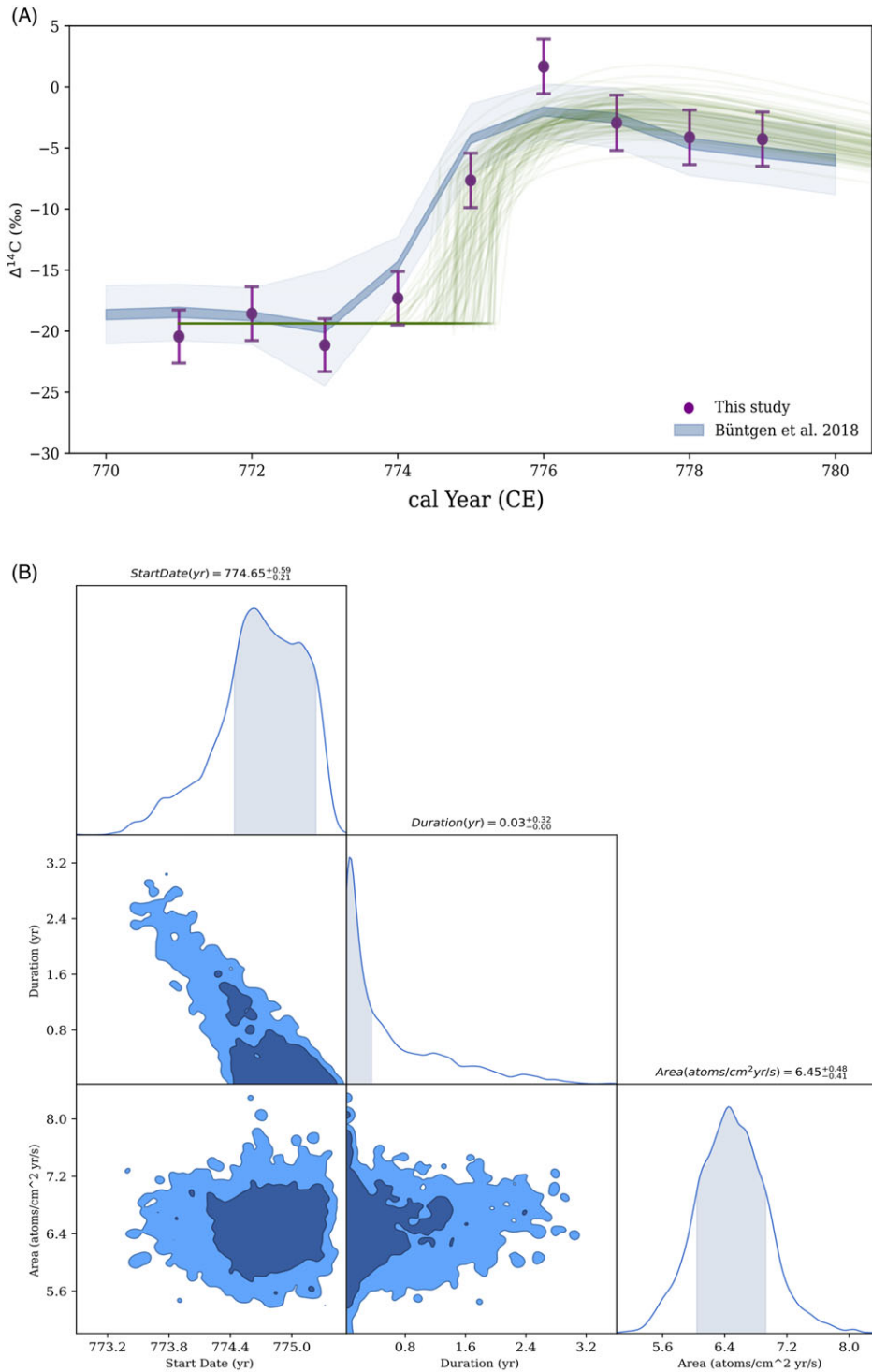


Figure 1. 775 CE Event. On the top (A), results of the ^{14}C analysis over the sample D1600030 and comparison with the results of Büntgen et al. (2018). The green lines are the ticktack model results. On the bottom (B), results of the ticktack analysis over the same dataset, showing the surface distribution of the modeled posterior parameters.

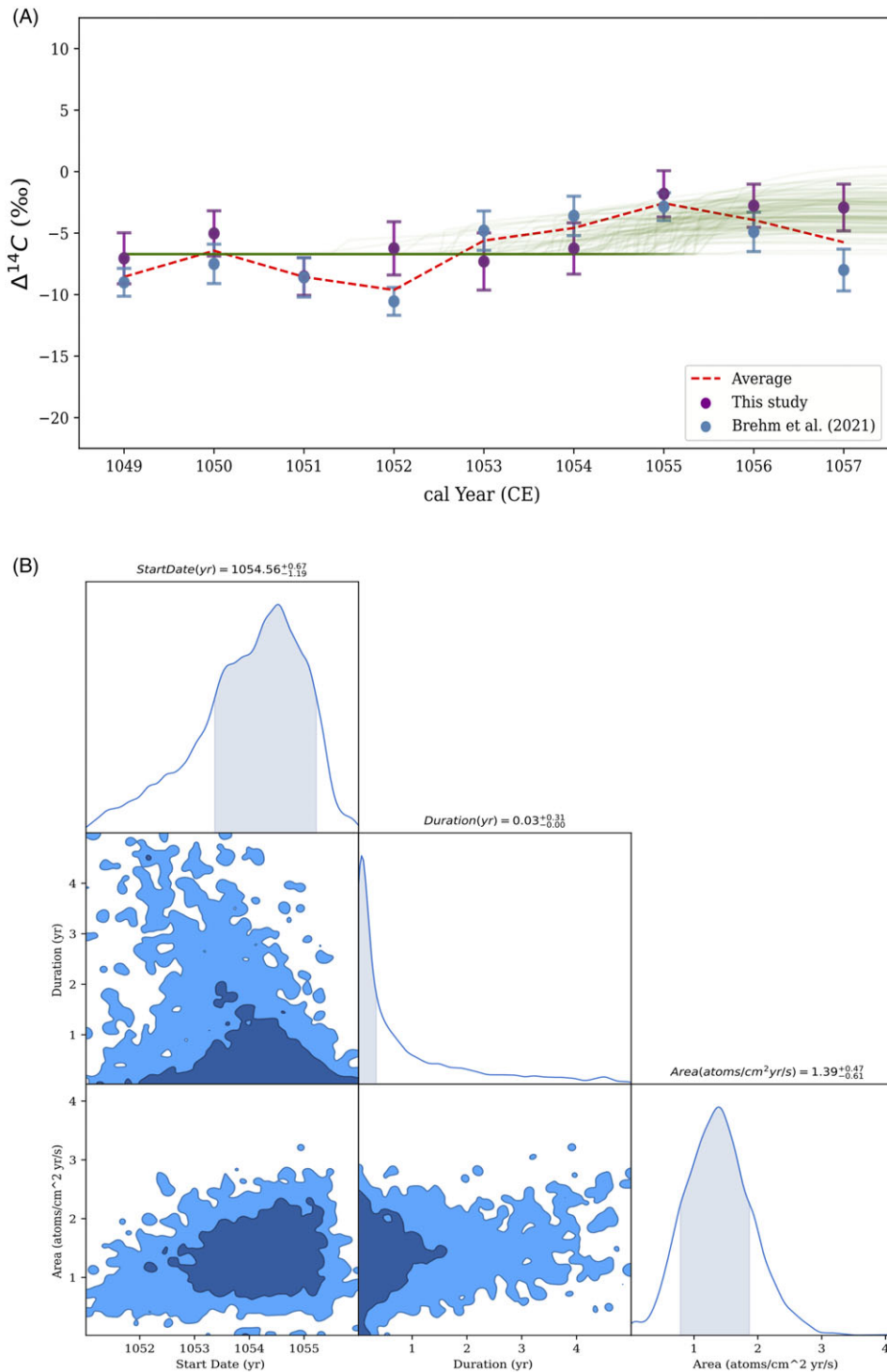


Figure 2. 1052 CE event candidate. On the top (A), results of the ^{14}C analysis over the sample BIF-E19 and comparison with the results of Brehm et al. (2021), and the average between the two datasets. The green lines are the ticktack model results. On the bottom (B), results of the ticktack analysis over the same dataset, showing the surface distribution of the modeled posterior parameters.

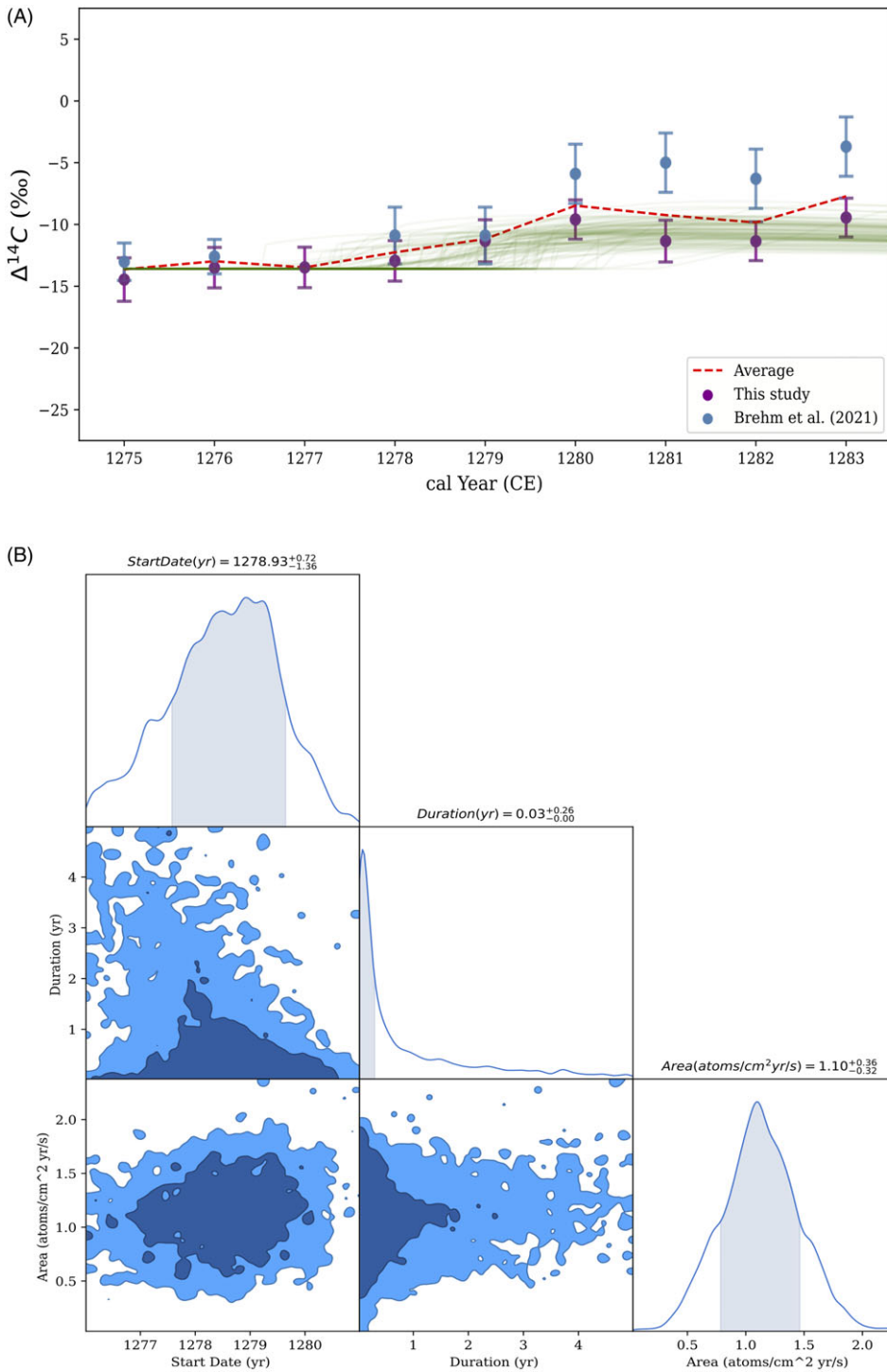


Figure 3. 1279 CE event candidate. On the top (A), results of the ^{14}C analysis over the sample APT-CO2 and comparison with the results of Brehm et al. (2021), and the average between the two datasets. The green lines are the ticktack model results. On the bottom (B), results of the ticktack analysis over the same dataset, showing the surface distribution of the modeled posterior parameters.

connection with an SEP event. Once more, all the data points of our time series agree with those of Brehm et al. (2021) at 1σ probability, apart from the last three at 1281, 1282 and 1283 CE. Again, all the sets of same-year measurements pass the χ^2 -test at 5% significance level, apart from the year 1281, which passes the test at 2.5% significance level. Thus, our results are again statistically compatible with Brehm et al. (2021), and both data sets can also be averaged (see Supplementary Information, SI2). Nevertheless, the increase reported in their study is not noticeable in this study, as between those years we report a change of just $1.7 \pm 1.6\%$. Alternatively, we could consider a time interval of 2 years, say between 1278 and 1280 CE, but even in that case the rise becomes only $3.3 \pm 1.6\%$. This latter value is in agreement with a recent analysis of the same event candidate (Miyahara et al. 2022).

Finally, we present a comparison case: new ^{14}C measurements over the time period from 531 to 550 CE (Figure 4A). This time series shows a relatively flat trend for the first 11 years, with a subsequent gradual and slow rise starting on year 541 CE. To reiterate, we do not observe a single-year rise in this data either. However, a relatively steep rise endures for several years, peaking in 546 CE. The magnitude of the rise, taken over the period from 541 to 546 CE, amounts to $6.3 \pm 1.6\%$, which is of a similar to the magnitude of the rise shown in the two previous examples, only on a multiple-year basis, as this signal could be part of an 11-year cycle.

To gain further insights into the possibility that real disturbances occurred in atmospheric $\Delta^{14}\text{C}$ levels over these time periods we need to take into account the ^{14}C cycle, employing a global CBM, and we do so by using of the *ticktack* package. This package passes the ^{14}C data through the chosen carbon box model, takes for granted that a ^{14}C production event happened within the dataset, and tries to best fit the ^{14}C production rate to the data varying its parameters. In the bottom part of each Figure, noted by the letter B, corner plots of the inferred parameters, directly produced by *ticktack*, are shown for each of the periods in question. In dark blue are the 68.2% likelihood intervals of highest posterior density, and in light blue the 95.4% likelihood intervals. In the upper part of each Figure, noted by the letter A, the green lines represent the results of the model expressed in terms of $\Delta^{14}\text{C}$. In our study we first perform a *ticktack* analysis applying the *spike only* method to the datasets presented in Table 1. Then we perform a second *ticktack* analysis applying the *flexible sinusoid affine variant* method. In order to allow a sinusoidal fit of approximately 11 years, the datasets need to be long enough to incorporate at least two full periods. As this was not possible with the new datasets presented in this study, we overcame this obstacle by analyzing additional datasets. For the 775 CE Event, we use the dataset originally published by Miyake et al. (2012). For the 1052 CE event candidate, we merge our dataset with the dataset from Eastoe et al. (2019), averaging those measurements corresponding to same growth years. We could not use the dataset from Brehm et al. (2021) as it has a gap between the years 1042 and 1049 CE. For the 1279 CE event candidate, the same procedure as above is done using the dataset from Brehm et al. (2021). For the 540s CE feature, we use the same datasets we used in the first analysis.

First, we show the results over the new measurements of the 775 Event (Figure 1B). The *spike only* analysis points to an increase in ^{14}C production of around 6.4 atoms/cm²/s per year, value that fits the estimate proposed by Gütler et al. (2015), with a start date estimated within the year 774 CE and an event duration that hits the minimum resolution of the model, which is around 11 days, hinting to an event duration of less than a month. All the 68.2% likelihood intervals are well constrained with a narrow margin around distinct values. Furthermore, the analysis of this event with the *flexible sinusoid affine variant* shows results in agreement with the *spike only* analysis (Figure 5-SI, Supplementary Information 4).

Second, we show the results over our new measurements of the 1052 CE event candidate (Figure 2B). The modeled increase in ^{14}C production to fit the data is in this case of just 1.4 atoms/cm²/s per year, with a start date estimated to be around the year 1054 CE, instead of the year 1052 showed by the data in Brehm et al. (2021), even though the 68.2% likelihood interval is less well defined, as it ranges from middle of year 1053 CE to the beginning of year 1055 CE. Event duration peaks again around the minimum resolution of the model, but with a larger spread, as in general all probability regions result more widespread. The analysis of this event with the *flexible sinusoid affine*

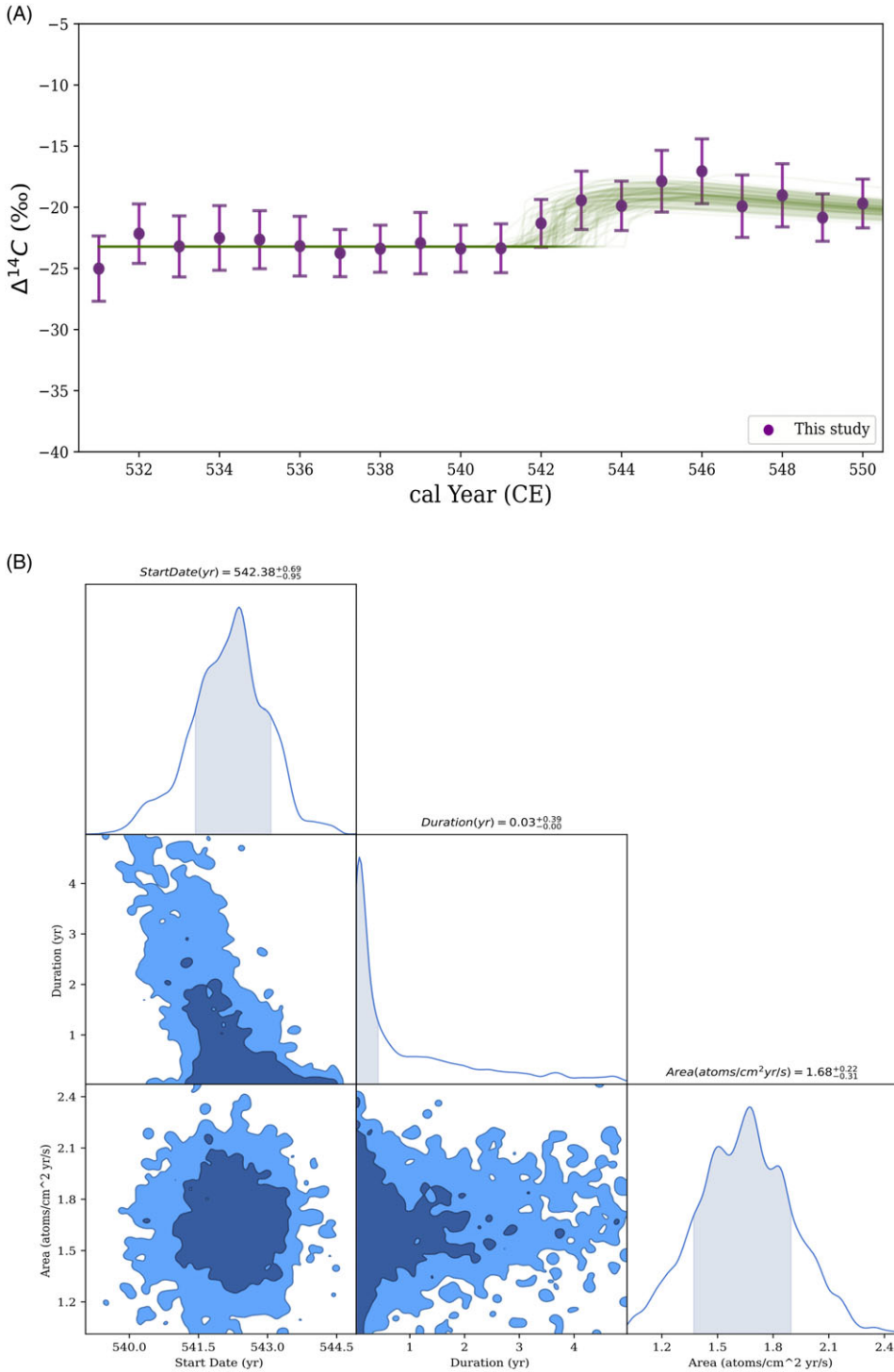


Figure 4. 540s ^{14}C feature. On the top (A), results of the ^{14}C analysis over the sample 14.0123.121. The green lines are the ticktack model results. On the bottom (B), results of the ticktack analysis over the same dataset, showing the surface distribution of the modelled posterior parameters.

variant shows an even lower estimated production rate, and an unresolved start date for the possible event (Figure 6-SI, Supplementary Information 4).

Third, we show the results over our new measurements of the 1279 CE event candidate (Figure 3B). The modeled increase in ^{14}C production to fit the data is in this case of just 1.1 atoms/cm²/s per year, with a start date estimated to be between 1277 and 1279 CE. The event duration peaks once again around the minimum resolution of the model, with again the 1 σ probability densities for Start Date and Event Duration being more widespread. Also in this case, the analysis of this event with the flexible sinusoid affine variant shows an even lower estimated production rate, and an unresolved start date for the possible event (Figure 7-SI, Supplementary Information 4).

Finally, we show the results over our new measurements of the ^{14}C feature around the years 540s CE (Figure 4B). In this case, the modeled increase in ^{14}C production is of 1.7 atoms/cm²/s per year, with a start date centered around year 542 CE and an event duration once more peaking around the minimum resolution of the model, but with the biggest time spread so far between these analyses, suggesting a possible long-lasting increase in ^{14}C production, that would match the longer rise seen in the data. Once more, the analysis of this event with the flexible sinusoid affine variant shows results in agreement with the spike only analysis (Figure 7-SI, Supplementary Information 4). The result of this analysis in terms of estimated production rate is comparable to those obtained in the two previous cases. However, the cause of this feature is to be deemed uncertain, as the small increase spreads over multiple years, where a normal change in solar modulation could explain the feature. However, a totally different phenomenon could be the cause of this increase; for instance, it has been shown that a major cooling event would reduce deep-water circulation, and such an occurrence can be associated with a higher atmospheric $^{14}\text{C}/^{12}\text{C}$ ratio (Goslar et al. 1995; Muscheler et al. 2008; Stocker and Wright 1996). Curiously, this rise in atmospheric $\Delta^{14}\text{C}$ coincides with coolest period in the Northern Hemisphere during the Common Era, widely attributed to volcanic eruptions in 536 and 540 CE (Sigl et al. 2015; Smith et al. 2020).

Comparing these different datasets and analyzes, a clear distinction can be made between the 775 CE event and the other analyzed time periods; the former can be clearly recognized as a sudden spike in $\Delta^{14}\text{C}$, as it corresponds to an increase in ^{14}C production rate of about 6.37 ^{14}C atoms/cm²/s (parameter “Area” from ticktack model), or 3 to 4 times the production rate in normal conditions (Kovaltsov et al. 2012). The other three features, while they still show an increase in $\Delta^{14}\text{C}$, only do so for a magnitude comparable to 1 or 2 times the measurement error of the baseline before the supposed event, and furthermore the estimated total excess ^{14}C production generated during these uplifts is less than double what would be expected from normal background cosmic radiation (Kovaltsov et al. 2012), and this could easily be caused by normal variations in solar modulation. Clearly all three periods do represent increases in the $^{14}\text{C}/^{12}\text{C}$ ratio in the atmosphere but there is scant evidence here for what might be described as an instantaneous production event, let alone a phenomenon comparable with a ^{14}C production event. Another point to be made is about reproducibility of results. The biggest global occurring SEP events, like the 775 CE and 994 CE events, are characterized, amongst other factors, by the fact they have roughly the same excursion signature detectable in tree rings from all over the world. In the case of these event candidates, the proposed signature is so minute that clear reproducibility between independent studies is unobtainable. For instance, as previously mentioned, Miyahara et al. (2022) reports the 1279 CE event candidate to be a $\Delta^{14}\text{C}$ increase of about 3‰ between the years 1279 and 1280 CE, instead of the 5‰ reported by Brehm et al. (2021), while in this study we report an increase of about 2‰. This means that between the studies, the same ^{14}C feature differs by up to 60% of the initially proposed value. When considering measurement errors and geographical variability, it appears evident that distinguishing lower magnitude events in the ^{14}C record is a challenging and uncertain task. We argue that some caution needs to be used when dealing with $\Delta^{14}\text{C}$ increases of this small magnitude, and we stress the importance of cross-checking every proposed event with additional analysis from other groups and samples, like in the case of this study. However, to resolve such small features, this may not be enough, as supporting evidence from ^{10}Be and ^{36}Cl data would be needed to definitively pinpoint the origin of these features, even though an additional challenge would be that for

such small features, such ice core data is often too noisy and poorly resolved, to properly detect them (Mekhaldi et al. 2021). Although we do not wholeheartedly challenge the existence of these features, we only question the attribution of their origin, as such excursions could be potentially be caused by normal changes in solar modulation or by other climatic phenomena.

Conclusions

In an attempt to replicate the results shown by Brehm et al. (2021) regarding the proposed event candidates of 1052 CE and 1279 CE, we measured and analyzed samples spanning the years concerned. Our results, despite being statistically consistent with the one published in the first study, do not show a clear change in $\Delta^{14}\text{C}$ from one year to the next. We suggest that such small increases in $\Delta^{14}\text{C}$ cannot be claimed as radiation events with absolute certainty on the basis of the current evidence, and certainly cannot be reliably used for exact-year dating, for two main reasons. Firstly, in order to confidently claim them as globally attested radiation events, the signature of their ^{14}C excursions should be clearly replicable from multiple studies, and from different datasets; however, the low magnitude of these features makes it challenging to distinguish unequivocally between the influence of production rate changes, the intrinsic variability of the measurement, and the geographically dependent variability of atmospheric $^{14}\text{C}/^{12}\text{C}$ ratio; furthermore, additional support from other cosmogenic isotopes analysis, such as ^{10}Be and ^{36}Cl , would be needed to support such hypotheses. Secondly, these excursions reflect a relatively small increase in ^{14}C production rate, which is very different from the increases demonstrated by the established extreme SEP events. Indeed, they are perhaps more compatible with divergences caused by environmental events, a different mechanism altogether, or by variations in solar modulation.

Supplementary material. To view supplementary material for this article, please visit <https://doi.org/10.1017/RDC.2024.52>

Acknowledgments. This work was supported by a European Research Council grant (ECHOES, 714679). We would like to acknowledge the contribution to this research of the staff at the Centre for Isotope Research, Groningen, especially M. Kuitems, A. Neocleous, A. Aerts-Bijma, S. de Bruijn, R. Linker, S. Palstra, R. Schellekens, J. Spiensma and D. van Zonneveld; the team of developers of the `ticktack` package, Q. Zhang, U. Sharma, J. Dennis and B. J. S. Pope; A. Arnold and R. Howard for dissecting the English tree-ring samples, and E. Jansma for dissecting the Dorestad sample.

References

- Aerts-Bijma AT, Paul D, Dee MW, Palstra SWL and Meijer HAJ (2021) An independent assessment of uncertainty for radiocarbon analysis with the new generation high-yield accelerator mass spectrometers. *Radiocarbon* **63**(1), 1–22.
- Beer J, McCracken K and von Steiger R (2012) Production of cosmogenic radionuclides in the atmosphere. In *Cosmogenic Radionuclides. Physics of Earth and Space Environments*. Berlin, Heidelberg: Springer, 139–177. https://doi.org/10.1007/978-3-642-14651-0_10.
- Brehm N, Bayliss A, Christl M, Synal H-A, Adolphi F, Beer J, Kromer B, Muscheler R, Solanki SK, Usoskin I et al (2021) Eleven-year solar cycles over the last millennium revealed by radiocarbon in tree rings. *Nature Geoscience* **14**(1), 10–15.
- Büntgen U, Eggertsson Ó, Wacker L, Sigl M, Ljungqvist FC, Di Cosmo N, Plunkett G, Krusic PJ, Newfield TP, Esper J et al (2017) Multi-proxy dating of Iceland’s major pre-settlement Katla eruption to 822–823 CE. *Geology* **45**(9), 783–786.
- Büntgen U, Wacker L, Galvan JD, Arnold S, Arseneault D, Baillie M, Beer J, Bernabei M, Bleicher N, Boswijk G et al (2018) Tree rings reveal globally coherent signature of cosmogenic radiocarbon events in 774 and 993 CE. *Nat Commun* **9**(1), 3605.
- Damon PE, Linick TW (1986) Geomagnetic-heliomagnetic modulation of atmospheric radiocarbon production. *Radiocarbon* **28**(2A), 266–278.
- Damon PE, Long A and Wallick EI. 1973. On the magnitude of the 11-year radiocarbon cycle. *Earth and Planetary Science Letters* **20**(3), 300–306.
- Dee M, Pope B, Miles D, Manning S and Miyake F (2016) Supernovae and single-year anomalies in the atmospheric radiocarbon record. *Radiocarbon* **59**(2), 293–302.
- Dee MW, Palstra SWL, Aerts-Bijma AT, Bleeker MO, de Bruijn S, Ghebru F, Jansen HG, Kuitems M, Paul D, Richie RR et al (2020). Radiocarbon dating at Groningen: new and updated chemical pretreatment procedures. *Radiocarbon* **62**(1), 63–74.
- Doeve P (2017) Dendrochronologische onderzoek Ruiselede waterputten (BAAC project 14.0123). V1 ed.: DataverseNL.
- Doeve P and Jansma E (2023) Dorestad, palen uit de haven. Projectnummer dendrochronologie (Stichting RING): 2016003. V2 ed.: DataverseNL.

- Eastoe CJ, Tucek CS and Touchan R (2019) $\Delta^{14}\text{C}$ and $\delta^{13}\text{C}$ in annual tree-ring samples from *sequoiadendron giganteum*, AD 998–1510: solar cycles and climate. *Radiocarbon* **61**(3), 661–680.
- Goodman J and Wearé J (2010) Ensemble samplers with affine invariance. *Communications in Applied Mathematics and Computational Science* **5**(1), 65–80.
- Goslar T, Arnold M, Bard E, Kuc T, Pazdur MF, Ralska-Jasiewiczowa M, Rozanski K, Tisnerat N, Walanus A, Wicik B et al 1995. High concentration of atmospheric ^{14}C during the Younger Dryas cold episode. *Nature* **377**(6548), 414.
- Güttler D, Adolphi F, Beer J, Bleicher N, Boswijk G, Christl M, Hogg A, Palmer J, Vockenhuber C, Wacker L et al 2015. Rapid increase in cosmogenic ^{14}C in AD 775 measured in New Zealand kauri trees indicates short-lived increase in ^{14}C production spanning both hemispheres. *Earth and Planetary Science Letters* **411**, 290–297.
- Jull AJT, Panyushkina IP, Molnár M, Varga T, Wacker L, Brehm N, Laszló E, Baisan C, Salzer MW and Tegel W (2021) Rapid ^{14}C excursion at 3372–3371 BCE not observed at two different locations. *Nature Communications* **12**(1), 712.
- Kovaltsov GA, Mishev A, Usoskin IG (2012) A new model of cosmogenic production of radiocarbon ^{14}C in the atmosphere. *Earth and Planetary Science Letters* **337–338**, 114–120.
- Kuitems M, Panin A, Scifo A, Arzhantseva I, Kononov Y, Doeve P, Neocleous A and Dee M (2020) Radiocarbon-based approach capable of subannual precision resolves the origins of the site of Por-Bajin. *Proc Natl Acad Sci U S A* **117**(25), 14038–14041.
- Kuitems M, Wallace BL, Lindsay C, Scifo A, Doeve P, Jenkins K, Lindauer S, Erdil P, Ledger PM, Forbes V et al (2022) Evidence for European presence in the Americas in AD 1021. *Nature* **601**(7893), 388–391.
- Lingenfelter RE (1963) Production of Carbon 14 by cosmic-ray neutrons. *Reviews of Geophysics* **1**(1), 35–55.
- McCracken KG, Dreschhoff GAM, Zeller EJ, Smart DF and Shea MA (2001) Solar cosmic ray events for the period 1561–1994: 1. Identification in polar ice, 1561–1950. *Journal of Geophysical Research: Space Physics* **106**(A10), 21585–21598.
- Mekhaldi F, Adolphi F, Herbst K and Muscheler R (2021) The signal of solar storms embedded in cosmogenic radionuclides: detectability and uncertainties. *Journal of Geophysical Research: Space Physics* **126**(8).
- Mekhaldi F, Muscheler R, Adolphi F, Aldahan A, Beer J, McConnell JR, Possnert G, Sigl M, Svensson A, Synal HA et al 2015. Multiradionuclide evidence for the solar origin of the cosmic-ray events of AD 774/5 and 993/4. *Nat Commun* **6**:8611.
- Melott AL and Thomas BC (2012) Causes of an AD 774/775 ^{14}C increase. *Nature* **491**(7426), E1–2.
- Miyahara H, Tokanai F, Moriya T, Takeyama M, Sakurai H, Ohyama M, Horiuchi K and Hotta H (2022) Recurrent large-scale solar proton events before the onset of the Wolf Grand Solar Minimum. *Geophysical Research Letters* **49**(5).
- Miyake F, Masuda K and Nakamura T (2013) Another rapid event in the carbon-14 content of tree rings. *Nat Commun* **4**:1748.
- Miyake F, Nagaya K, Masuda K and Nakamura T (2012) A signature of cosmic-ray increase in AD 774–775 from tree rings in Japan. *Nature* **486**(7402), 240–242.
- Muscheler R, Kromer B, Björck S, Svensson A, Friedrich M, Kaiser KF and Southon J (2008) Tree rings and ice cores reveal ^{14}C calibration uncertainties during the Younger Dryas. *Nature Geoscience* **1**(4), 263–267.
- Nakamura T, Nakai N and Ohishi S (1987) Applications of environmental ^{14}C measured by AMS as a carbon tracer. *Nuclear Instruments and Methods in Physics Research B* **29**(1), 235–260.
- O'Hare P, Mekhaldi F, Adolphi F, Raisbeck G, Aldahan A, Anderberg E, Beer J, Christl M, Fahrni S, Synal H-A et al (2019) Multiradionuclide evidence for an extreme solar proton event around 2,610 B.P. (~660 BC). *Proceedings of the National Academy of Sciences* **116**(13), 5961–5966.
- Oeschger H, Siegenthaler U, Schotterer U and Gugelmann A (1975) A box diffusion model to study the carbon dioxide exchange in nature. *Tellus* **27**(2), 168–192.
- Oppenheimer C, Wacker L, Xu J, Galván JD, Stoffel M, Guillet S, Corona C, Sigl M, Di Cosmo N and Hajdas I et al (2017) Multi-proxy dating the “Millennium Eruption” of Changbaishan to late 946 CE. *Quaternary Science Reviews* **158**, 164–171.
- Paleari CI, Mekhaldi F, Adolphi F, Christl M, Vockenhuber C, Gautschi P, Beer J, Brehm N, Erhardt T and Synal H-A et al (2022) Cosmogenic radionuclides reveal an extreme solar particle storm near a solar minimum 9125 years BP. *Nature Communications* **13**(1), 214.
- Paleari CI, Mekhaldi F, Erhardt T, Zheng M, Christl M, Adolphi F, Hörhold M and Muscheler R (2023) Evaluating the 11-year solar cycle and short-term ^{10}Be deposition events with novel excess water samples from the East Greenland Ice-core Project (EGRIP). *Clim Past* **19**(11), 2409–2422.
- Panyushkina I, Livina V, Molnár M, Varga T and Jull AJT (2022) Scaling the ^{14}C -excursion signal in multiple tree-ring series with dynamic time warping. *Radiocarbon* **64**(6), 1587–1595.
- Pavlov AK, Blinov AV, Konstantinov AN, Ostryakov VM, Vasilyev GI, Vdovina MA and Volkov PA (2013) AD 775 pulse of cosmogenic radionuclides production as imprint of a Galactic gamma-ray burst. *Monthly Notices of the Royal Astronomical Society* **435**(4), 2878–2884.
- Pedro JB, McConnell JR, van Ommen TD, Fink D, Curran MAJ, Smith AM, Simon KJ, Moy AD and Das SB (2012) Solar and climate influences on ice core ^{10}Be records from Antarctica and Greenland during the neutron monitor era. *Earth and Planetary Science Letters* **355–356**, 174–186.
- Scifo A, Kuitems M, Neocleous A, Pope BJS, Miles D, Jansma E, Doeve P, Smith AM, Miyake F and Dee MW (2019) Radiocarbon production events and their potential relationship with the Schwabe Cycle. *Sci Rep* **9**(1), 17056.
- Siegenthaler U, Heimann M and Oeschger H (1980) ^{14}C variations caused by changes in the global carbon cycle. *Radiocarbon* **22**(2), 177–191.
- Sigl M, Winstrop M, McConnell JR, Welten KC, Plunkett G, Ludlow F, Buntgen U, Caffee M, Chellman N and Dahl-Jensen D et al (2015) Timing and climate forcing of volcanic eruptions for the past 2,500 years. *Nature* **523**(7562), 543–549.
- Simpson JA (1951) Neutrons produced in the atmosphere by the cosmic radiations. *Physical Review* **83**(6), 1175–1188.

- Smart DF, Shea MA and McCracken KG (2006) The Carrington event: Possible solar proton intensity–time profile. *Advances in Space Research* **38**(2), 215–225.
- Smith VC, Costa A, Aguirre-Diaz G, Pedrazzi D, Scifo A, Plunkett G, Poret M, Tournigand PY, Miles D and Dee MW et al (2020) The magnitude and impact of the 431 CE Tierra Blanca Joven eruption of Ilopango, El Salvador. *Proc Natl Acad Sci U S A* **117**(42), 26061–26068.
- Stocker TF and Wright DG (1996) Rapid changes in ocean circulation and atmospheric radiocarbon. *Paleoceanography* **11**(6), 773–795.
- Stuiver M (1961) Variations in radiocarbon concentration and sunspot activity. *Journal of Geophysical Research* **66**(1), 273–276.
- Stuiver M, Braziunas TF (1993) Sun, ocean, climate and atmospheric ^{14}C : an evaluation of causal and spectral relationships. *The Holocene* **3**(4), 289–305.
- Terrasi F, Marzaioli F, Buompane R, Passariello I, Porzio G, Capano M, Helama S, Oinonen M, Nöjd P and Uusitalo J et al (2020) Can the ^{14}C production in 1055 CE be affected by SN1054? *Radiocarbon* **62**(5), 1403–1418.
- Usoskin IG (2017) A history of solar activity over millennia. *Living Reviews in Solar Physics* **14**(1).
- Usoskin IG, Koldobskiy SA, Kovaltsov GA, Rozanov EV, Sukhodolov TV, Mishev AL and Mironova IA (2020) Revisited reference solar proton event of 23 February 1956: Assessment of the cosmogenic-isotope method sensitivity to extreme solar events. *Journal of Geophysical Research: Space Physics* **125**(6).
- Usoskin IG, Kromer B, Ludlow F, Beer J, Friedrich M, Kovaltsov GA, Solanki SK and Wacker L (2013) The AD775 cosmic event revisited: the Sun is to blame. *Astronomy & Astrophysics* **552**.
- Wacker L, Güttler D, Synal H-A, Walti N, Goll J and Hurni JP (2014) Radiocarbon dating to a single year by means of rapid atmospheric ^{14}C changes. *Radiocarbon* **56**(2), 573–579.
- Wang FY, Yu H, Zou YC, Dai ZG and Cheng KS (2017) A rapid cosmic-ray increase in BC 3372–3371 from ancient buried tree rings in China. *Nat Commun* **8**(1), 1487.
- Webber WR, Higbie PR and McCracken KG (2007) Production of the cosmogenic isotopes ^3H , ^7Be , ^{10}Be , and ^{36}Cl in the Earth's atmosphere by solar and galactic cosmic rays. *Journal of Geophysical Research: Space Physics* **112**(A10).
- Wolff EW, Bigler M, Curran MAJ, Dibb JE, Frey MM, Legrand M and McConnell JR (2012) The Carrington event not observed in most ice core nitrate records. *Geophysical Research Letters* **39**(8).
- Zhang Q, Sharma U, Dennis JA, Scifo A, Kuitems M, Büntgen U, Owens MJ, Dee MW and Pope BJS (2022) Modelling cosmic radiation events in the tree-ring radiocarbon record. *Proceedings of the Royal Society A: Mathematical, Physical and Engineering Sciences* **478**(2266).